HYPERSPECTRAL IMAGING FOR PEACH RIPENING ASSESSMENT

L. Lleó[1], B. Diezma-Iglesias[3], J.M. Roger[2], A. Herrero-Langreo[3]

[1]Departamento de Ciencia y T. A. a la I. Técnica Agrícola, E. U. I. T. A., 28040 Madrid, Spain.
[2]CEMAGREF, 361 rue Jean-François Breton BP 5095, 34196 Montpellier Cedex 5, France.
[3]Physical Properties and Advanced Techniques in Agrofood, LPF-TAG Rural Engineering Dept, Universidad Politécnica de Madrid, c/Ciudad Universitaria s/n, 28040 Madrid, Spain
lourdes.lleo@ upm.es

Abstract

The present research is focused on the application of artificial vision to peach ripening assessment, avoiding multiplicative and additive effect. Original images were acquired with a hyperspectral camera. Vision allows a spatially detailed determination of the ripening stage of the fruit. Optical indexes are proposed, based on the combination of wavelengths close to the chlorophyll absorption peak at 680 nm. Ind1 corresponds approximately to the depth of the absorption peak, and Ind_2 corresponds to the relative absorption peak. An artificial image of each index was obtained by computing the corresponding reflectance images. Score images have been also computed from Principal Components and Partial Least Squares Analysis. In any case the best performances correspond to such images that correct multiplicative and additive effects. Ind_2 is the preferred index; it showed the highest discriminating power between ripening stages and no influence of convexity. Ind_2 also allowed the differentiation of ripening regions within the fruits, and it showed the evolution of those regions during ripening. This fact has been also observed in some of the score images.

Keywords - Image Analysis, Ripeness, Quality, Vision.

INTRODUCTION

The quality assessment of fruits, particularly of peaches, is important for establishing the optimal harvest date and the best postharvest treatment, storage temperature and the delay before consumption. Peaches do not ripen in a homogeneous way. Depending on the cultivar, different areas of the fruit (e.g., the tip and shoulders) soften faster than others, and, therefore, these areas are more susceptible to damage and disease [1]. Consequently, there is a need to develop non-destructive measuring techniques such as vision, which can provide a spatially detailed measurement of the degree of ripeness. When assessing ripening with vision, it is crucial to identify the spectral changes associated with pigment evolution during ripening. Chlorophyll is the most important pigment associated with ripening and it presents an absorption peak at 680 nm. As the fruit ripens, the reflection in this band increases due to chlorophyll degradation. Indexes, ratios or differences of wavelengths are used for avoid variable irradiance, background and geometric effects, etc. [2]. Several authors have studied different spectral indexes related to fruit ripening [3, 4]; and to peach maturity: index of absorbance difference, $I_{AD}= A_{670}-A_{720}$, [5]; the reflectance ratio 670 nm/800 nm [6].

The present research is focused on the application of artificial vision to peach ripening assessment, avoiding multiplicative and additive effect. The region of interest (the fruit) was previously segmented from the background using the Otsu method.Two main groups of artificial ripening images have been computed and compared:

A) First group of images corresponded to indexes or combinations of wavelengths around chlorophyll absorption peak (Ind_1, Ind_2, $Ind_3=R_{675}/R_{800}$ and I_{AD}).

B) Second group are images scores obtained from PCA, PLS computed on 1) a learning set of raw spectra extracted from equatorial area of the fruits (n=1069 spectra before ripening, n=1134 after ripening, 2) the same learning set of spectra, but pre-treated in order to avoid multiplicative (Standard Normal Variate, SNV) and additive (Savitsky Golay algorithm) effect. The images scores are the resulting inner product of the pixels of the raw images by the loadings obtained from the learning set.

Five commercially mature fruits (red-skinned, soft-flesh 'Richlady') were selected by expert assessment based on apparent colour and firmness. Hyperspectral images (HYSPEX VNIR 1,600-pixel push-broom camera, Hyspex, Norsk Elektro Optikk AS, Norway) of the selected fruits were acquired before and after the following ripening process: refrigerated storage for four days at 10ºC and ripening for three days at room temperature (20ºC). Two images were acquired per fruit and therefore a total of 18-20 images are analysed.

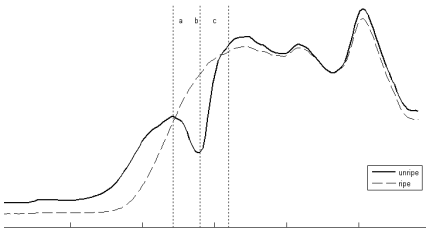

Fig. 1. Example of two reflectance spectra belonging to two different peaches: one unripe, which presents an absorption peak at 680 nm; and one ripe, which does not present any peak at 680 nm. The X axis corresponds to the wavelengths (nm). The Y axis corresponds to the reflectance level of the spectra (arbitrary units). The main difference is the chlorophyll absorption hole (around 680 nm), which disappears as the fruit ripens. Nevertheless, the apparent reflectance is affected by two phenomena. 1) A multiplicative effect due to variations of light scattering, which induce variations in the mean light path length. 2) An additive variation, due to some kind of specular reflection.

Next, the retrieval of the true reflectance involves two corrections that are respectively related to the multiplicative and additive effects; 1) a normalisation that consists of dividing the spectrum by a quantity that is affected by the multiplicative effect, 2) a baseline subtraction that consists of removing the background trend from each spectrum. The second order of differentiation is usually preferred because it removes the linear baselines and magnifies the peaks. The application of such corrections to the chlorophyll peak with a limited number of wavelengths can be achieved on the basis of three reflectances: R_a (640 nm), R_c (730 nm) and R_b (680 nm). These reflectances correspond respectively to the sides and the bottom of the peak, as illustrated in Figure 1. Two levels of correction can be applied, yielding two indexes:

- the baseline correction should be carried out by an approximation of the second derivative on the peak, as performed by Ind_1: $Ind_1 = R_a + R_c - 2R_b$

- the correction for the multiplicative effect is done in Ind_2 by dividing Ind_1 by the mean value of the two reflectances R_a and R_c (which should not depend on the ripening): $Ind_2 = (R_a + R_c - 2R_b) / ((R_a+R_c) / 2)$. After the simplification (dividing the numerator and denominator by R_a+R_c) and the removal of the constant terms, Ind_2 becomes: $Ind_2 = R_b / (R_a+R_c)$

RESULTS

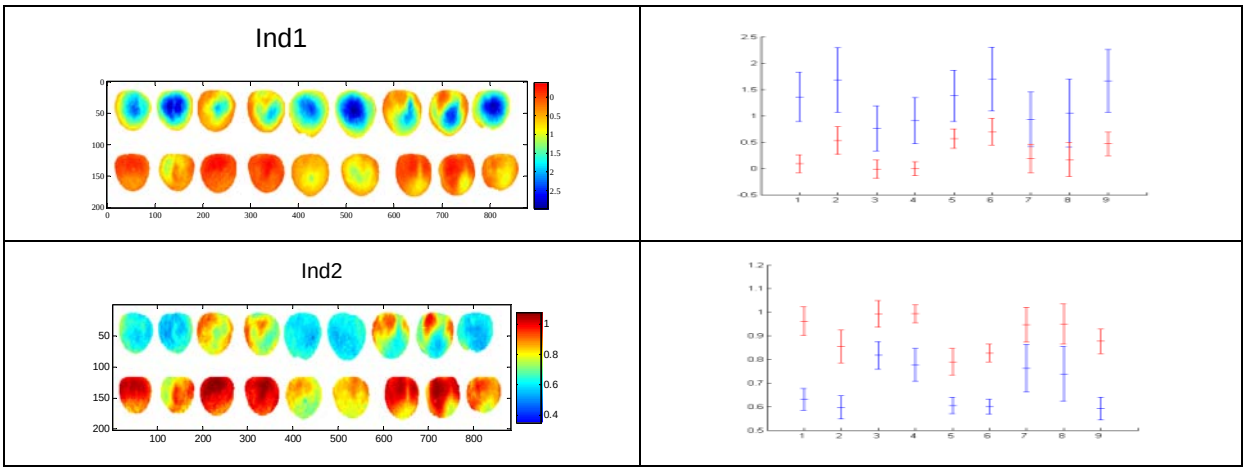

Figure 2. Lines 1 and 2 correspond to Ind1 and Ind2. Left column: reflectance images for fruits before, (first line of the image) and after ripening process (second line). Blue color corresponds to unripest areas or fruits and red to the ripest. Color bars of the figures indicate the scale of the values. Right column: averages plus minus standard deviation within the fruit; 'x' axis represents each fruit; 'y' axis represents the value of the index. Blue vertical lines correspond to the fruits before ripening and red lines to the same fruits after ripening process. Ind_1 decreased with maturity as expected. It also showed a certain convexity effect, which disappeared after ripening. Also, the variability within fruits decreased in non ripened fruits images when compared to ripened fruits images. The vertical lines blue and red show parallel evolution; the original maturity of the fruits could determine fruit ripening at the end of the process (Figure 2). Additionally, Ind_2 presented the lowest variability within fruits. The blue and red lines were completely parallel. Some ripened regions, on the top, near the shoulders, were allocated in the same areas before and after ripening. Intensity values and area increased after ripening, as can be observed in the third, fourth, seventh and eighth fruits from left to right, on the top of the fruit (Figure 2).

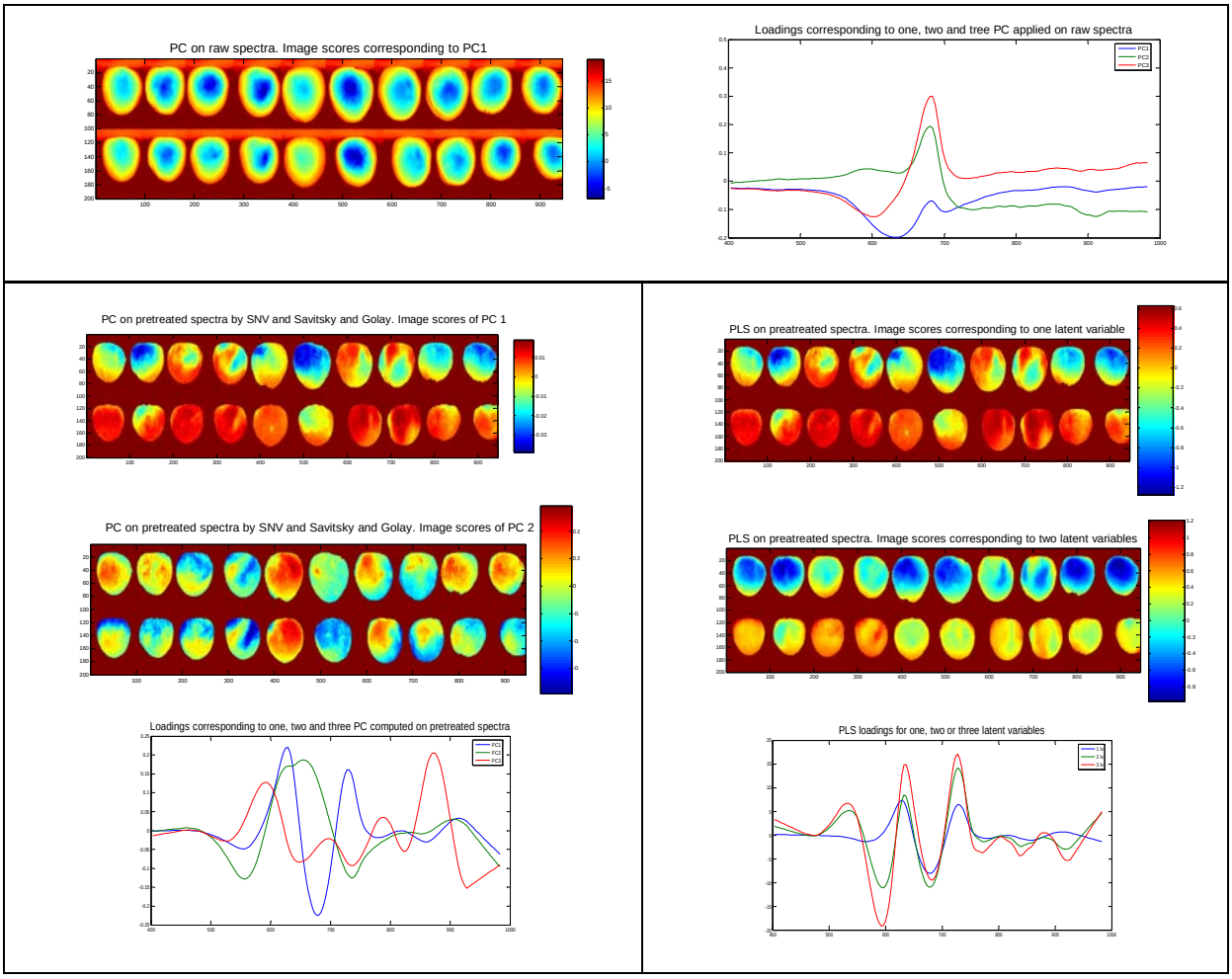

Fig.3. Score images are obtained from the projection of the hyperspectral raw or pretreated images onto PC's, or latent variables subspaces. First row left, score images obtained from PC applied on raw spectra (PC1); on the right the corresponding PC loadings. Second and third line left, score images from PC1 and PC2 applied on the pretreatred learning set (xndd). Fourth line left loadings of the PC corresponding to xndd. Second and third line right, score images from PLS with one and two latent variables on xndd. Fourth line right, the loadings of PLS corresponding to one, two and three latent variables on pretreatred spectra xndd.

PC1 and PC2 score images (not shown) corresponding to raw spectra present a high influence of the convexity of the fruit. It is not useful for ripening assessment since it appear no differences between

stages. Once the additive and multiplicative effects are corrected on the learning set, and also on the hyperspectral images, the corresponding score images present better performance. PC image scores (PC1 of pretreated images distinguish between ripening stages for each pair of fruits.

Both, PC1 and PLS with one latent variable, distinguish between fruits, between ripening stages, and they also identify regions inside the fruit that evolve after ripening. If they are compared with Ind_2, similar behaviour can be detected; all of them have been corrected from multiplicative and additive effect. Regarding loadings (from PC1 and PLS-one latent variable), the higher values correspond to the same wavelengths involved in the computation of Ind_2. However, in PC2 score image and PLS with three or more latent variables (not shown), the effect of ripening is less evident, and their corresponding loadings show high values for regions of the spectrum not clearly related to ripening evolution, such as near infrared. Wilks' lambda Λ (Wilks, 1960) was computed for each pair of fruits before and after ripening as the ratio between the inter-group variance and the residual variance. A high lambda value supposes high variance before and after ripening compared to the variability within fruits and, therefore, the corresponding index will have a higher discriminating power between the ripening stages. Nine pairs of fruits were considered, and thus, nine values of Λ were obtained per index and per type of scores. The objective of this analysis was to determine which artificial image better discriminate the ripening process.

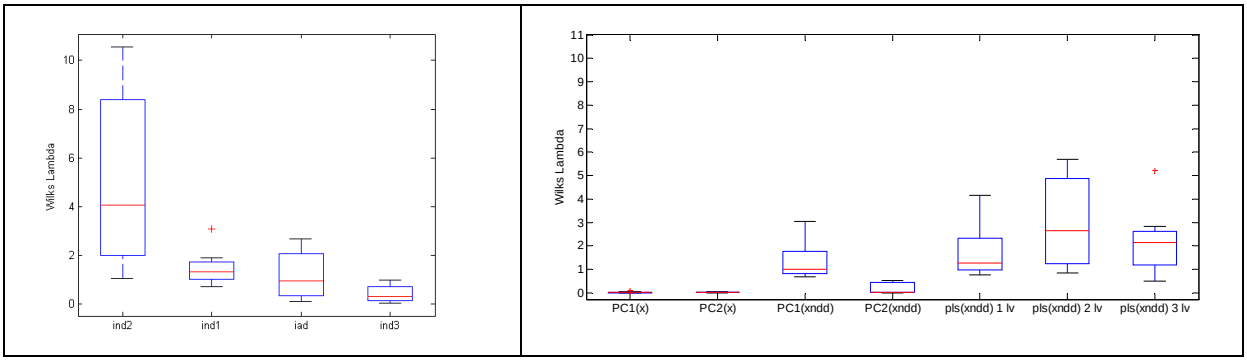

Fig.4. On the left, Wilks' lambda Λ inter-quartile ranges for the nine fruits before and after ripening (y axis) for the four indexes (x axis). Median values are indicated by horizontal lines in the boxes. The whole range is indicated by the whiskers. On the right, Wilks' lambda value for each fruit and index before and after ripening. Bold case indicates the lowest Λ, whereas cursive case indicates the highest Λ.

Ind_2 presented the highest median of lambda (Λ=4) following by pls on xndd with 2 latent variables (lv), (Λ=2,64), pls with three lv, (Λ=2,1), Ind_1 (Λ=1,5), etc. Furthermore Ind_2 always produced the highest Λ in the nine pair of fruits (not shown). In addition, PC1 and PC2 on raw spectra presented the worst discrimination ability.

CONCLUSIONS

The present research proposes several procedures for generating artificial images in order to discriminate ripening stage of fruits. Also it is proposed a method to compare and evaluate these images regarding the discrimination power, based on Wilks' lambda computation. These procedures could be applied to other kind of images and features, for discrimination or segregation of samples.

REFERENCES

[1] Crisosto, C. H., Slaughter, D. C., Garner, D. & Boyd, J. (2001). Stone fruits critical bruising thresholds. Journal American Pomological Society 55(2), 76-81.

[2] Xue, L. & Yang, L. (2009). Deriving leaf chlorophyll content of green-leafy vegetables from hyperspectral reflectance. ISPRS Journal of Photogrammetry and Remote Sensing, 64(1), 97-106.

[3] Zude, M. (2003). Comparison of indices and multivariate models to non-destructively predict the fruit chlorophyll by means of visible spectrometry in apple fruit. Analytica Chimica Acta, 481(1), 119-126

[4] Qin, J.; Lu, R. (2008). Measurement of the optical properties of fruits and vegetables using spatially. resolved hyperspectral diffuse reflectance imaging technique. Postharvest Biology and Technology, 49, 355–365

[5] Ziosi, V., Noferini, M., Fiori, G., Tadiello, A., Trainotti, L., Casadoro, G. & Costa, G. (2008). A new index based on vis spectroscopy to characterize the progression of ripening in peach fruit. Postharvest Biology and Technology, 49(3), 319-329.

[6] Lleó, L., Barreiro, P., Ruiz-Altisent, M. & Herrero, A. (2009). Multispectral images of peach related to firmness and maturity at harvest. Journal of Food Engineering, 93(2), 229-235.